Supporting Information

Formation of a tris(catecholato) iron(III) complex with a nature-inspired cyclic peptoid ligand

Jinyoung Oh,§[a] Dahyun Kang,§[a] Sugyeong Hong,[b] Sun H. Kim,[b] Jun-Ho Choi [a] and Jiwon Seo *[a]

[a]Department of Chemistry, School of Physics and Chemistry, Gwangju Institute of Science and Technology, 123 Cheomdangwagi-ro, Buk-gu, Gwangju, 61005, Republic of Korea.

[b]Western Seoul Center, Korea Basic Science Institute, University-Industry Cooperation Building, 150 Bukahyun-ro, Seodaemun-gu, Seoul, 120-140, Republic of Korea.

*jseo@gist.ac.kr (J. Seo)

§These authors contributed equally to this work.

Table of Contents

1. Experimental techniques and methods

a. Abbreviations

Acetonitrile (ACN); benzotriazole-1-yl-oxy-*tris*-pyrrolidino-phosphonium hexafluoro phosphate (PyBOP); *tert*-butoxycarbonyl (Boc); *N-N'*-dicyclohexylcarbodiimide (DCC); *N,N*-diisopropyl carbodiimide (DIC); *N,N*-diisopropylethylamine (DIEA); *N,N'*-dimethylformamide (DMF); *N,N'*-dimethylsulfoxide (DMSO); ethylemediaminetetraacetic acid (EDTA); 9-fluorenylmethoxyl carbonyl (Fmoc); 1-hydroxybenzotriazole hydrate (HOBt); 3-hydroxytyramine (dopamine); *N*-methyl-2-pyrrolidone (NMP); tetrahydrofuran (THF); trifluoroacetamide (Tfa); trifluoroacetic acid (TFA); 2,2,2-trifluoroethanol (TFE); triisopropylsilane (TIS).

b. General Methods

All reagents were purchased from Sigma-Aldrich (St. Louis, MO, USA), Alfa Aesar (Ward Hill, MA, USA), Novabiochem (Merck KGaA, Darmstadt, Germany) or TCI (Tokyo, Japan), and they were used without further purification. Microwave-assisted synthesis of peptoids was performed on a CEM MARS multimodal microwave reactor equipped with a magnetic stirrer and a fiber-optic temperature probe (CEM Corp., Matthews, NC, USA). Peptoid oligomers were analyzed by a Waters HPLC system. The Waters HPLC was equipped with a reverse-phase column (SunFire C18, 4.6 × 250 mm, 5 μm), Waters 2489 UV/Visible detector, Waters 1525 Binary HPLC Pump, Waters 2707 Autosampler and Waters 5CH column oven. The mobile phases were water (A, +0.1% TFA) and ACN (B, +0.1% TFA). At 40 ℃, before sample was injected, the column was conditioned with 5% B for 10 min. After sample was injected, 5% B was kept for 2 min. The linear gradient of 5-100% B was applied over 30 min at a flow rate of 1 mL/min. UV/visible detector was set to monitor sample elution at 220 nm. Peptoid oligomers were purified by a preparative HPLC system (Waters PrepLC system, Waters 2489 UV/Visible detector, Waters fraction collector III) using C18 columns (SunFire C18, 19 × 150 mm, 5 μm and Phenomenex C18, 21.2 × 250 nm, 5 μm) at a flow rate of 14 mL/min. Sample elution was monitored by detection absorbance at 220 nm. The purity of the product fractions was confirmed by analytical HPLC, and fractions containing pure product (>98% purity) were collected, lyophilized and stored at –80 °C. Mass data of peptoids were obtained from an Agilent LC/MS system which was equipped with 1260 Infinity LC and 6120 SQ bundle system with API-electrospray ion source.

c. Catechol-based peptoid submonomer synthesis.

Scheme S1. Synthesis of dopamine(acetonide)[1]

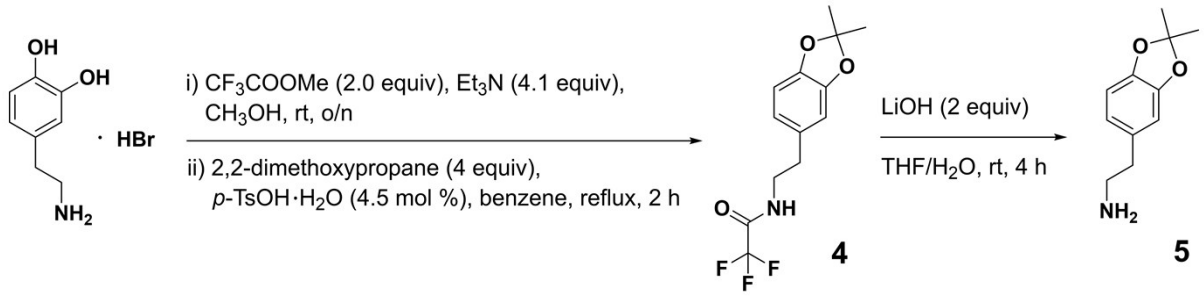

Tfa-dopamine(acetonide) (4). To a solution of 3-hydroxytyramine hydrobromide (10.0 g, 42.7 mmol) in MeOH (95.0 mL) was prepared under a nitrogen atmosphere. Then methyl trifluoroacetate (11.2 g, 87.2 mmol, 8.77 mL) and Et_3N (17.7 g, 175 mmol, 24.4 mL) was added. The reaction solution was stirred overnight at room temperature. The mixture was concentrated under vacuum. The residue was treated with 1 M HCl to pH = 1 and extracted by ethyl acetate. The organic layer was washed with water, dried over Na_2SO_4, filtered and concentrated to yield Tfa-dopamine. To a solution of Tfa-dopamine (10.3 g, 41.1 mmol) in benzene (411 mL), was added 2,2-dimethoxypropane (12.9 g, 123 mmol, 15.1 mL) into a 1 L two-neck flask. The reaction mixture was degassed with nitrogen and then refluxed by using a Soxhlet extractor. Then *p*-toluenesulfonic acid monohydrate (352 mg, 1.85 mmol, 4.5 mol %) was added. The reaction was determined by thin-layer chromatography (TLC). After 4 h, the reaction mixture was cooled down and filtered through a short silica-gel column using CH_2Cl_2. The organic mixture was concentrated under vacuum to give a light yellow solid. The pure product was recrystallized in CH_2Cl_2/*n*-hexane to yield 9.27 g (32.0 mmol, 75%) as a white crystal. R_f = 0.6 (CH_2Cl_2). ^{1}H NMR (400 MHz, $CDCl_3$) δ 6.68-6.57 (3H, m), 6.25 (1H, br s), 3.57 (2H, q, *J* = 6.56 Hz), 2.78 (2H, t, *J* = 6.87 Hz), 1.67 (6H, s).

Dopamine(acetonide) (6). To a solution of TFA-dopamine(acetonide) (9.53 g, 33.0 mmol) in THF (194 mL) was added a 1.03 M solution of LiOH (1.58 g, 65.9 mmol) in water (64.0 mL). The reaction mixture was stirred at room temperature for 4 h. The reaction was determined by thin-layer chromatography (TLC). The organic solvents were concentrated under vacuum, and the residue was treated carefully with 1 M HCl to pH = 8 and extracted with EtOAc. The organic layer was dried over Na_2SO_4, concentrated vacuum and purified by silica gel column chromatography. (CH_2Cl_2/MeOH/Et_3N = 8:1:0.1, v/v/v) to yield 5.22 g (27.0 mmol, 82%) as a light yellow oil. R_f = 0.33 (CH_2Cl_2/MeOH/Et_3N = 8:1:0.1). ^{1}H NMR (400 MHz, $CDCl_3$) δ 6.65-6.58 (3H, m), 5.31 (2H, br s), 3.06 (2H, t, *J* = 7.33 Hz), 2.82 (2H, t, *J* = 7.48 Hz), 1.64 (6H, s). The NMR spectrum of the final submonomer product was confirmed with the previous report.[1]

Scheme S2. Synthesis of *N*-(aminoethyl)-2,3-bis(benzyloxy)benzamide[2,3]

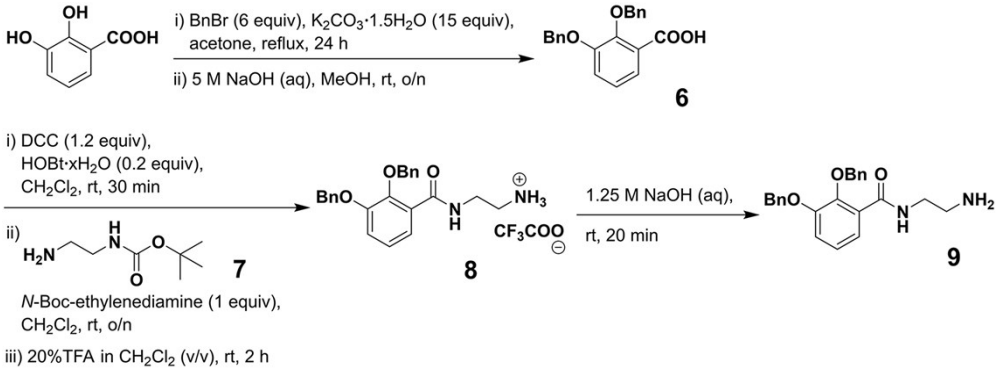

2,3-Bis(benzyloxy)benzoic acid (6). To a solution of 2,3-dihydroxybenzoic acid (3.08 g, 20 mmol), benzyl bromide (14.3 mL, 120 mmol), and $K_2CO_3 \cdot 1.5H_2O$ (49.6 g, 300 mmol) were prepared in acetone (400 mL) under a nitrogen atmosphere. Then the reaction solution was refluxed at room temperature for 24 h. The mixture was filtered and the filtrate was concentrated under vacuum to give a crude as a clear oil. The crude oil was dissolved in MeOH (1.24 L) and a 5.0 M solution of NaOH (300 mL) was added. The reaction mixture was refluxed for 3 h. The reaction was determined by thin-layer chromatography (TLC). The organic solvent was concentrated under vacuum. The residue was dissolved in water and washed with *n*-hexane. Then the water phase was acidified with 3 M HCl to pH = 2 and filtered to yield 6.6 g (19.7 mmol, 98%) as a white solid. R_f = 0.44 (acetone/*n*-hexane = 2:3); ^{1}H NMR (400 MHz, $CDCl_3$) δ 7.74-7.16 (13H, m), 5.25 (2H, s), 5.18 (2H, s).

***tert*-Butyl (2-aminoethyl)carbamate (7).** To a solution of di-*tert*-butyldicarbonate (10.5 g, 48.1 mmol) in CH_2Cl_2 (78.7 mL) was added dropwise to a solution of ethylenediamine (27.0 g, 449 mmol, 30.0 mL) in CH_2Cl_2 (167 mL) for 30 min. The reaction mixture was stirred under a nitrogen atmosphere at room temperature for 18 h. The reaction mixture was filtered, gently washed with water, and dried with Na_2SO_4. The organic layer was concentrated under vacuum to yield 3.9 g as light-yellow oil and used without further purification. (mixture of mono-Boc protected and di-Boc protected ethylenediamine)

2-(2,3-Bis(benzyloxy)benzamido)ethan-1-aminium trifluoroacetate (8). To a solution of **6** (4.98 g, 14.9 mmol), DCC (3.69 g, 17.9 mmol) and $HOBt \cdot xH_2O$ (0.423 g, 3.13 mmol) in CH_2Cl_2 (231 mL) was stirred at room temperature for 30 min and **9** (2.39 g, 14.9 mmol) was added. The reaction mixture was stirred overnight and filtered. The filtrate was washed with water and dried over Na_2SO_4. The organic layer was concentrated to give a crude yellowish oil. To a solution of crude oil in CH_2Cl_2 (30.0 mL) was cooled to 0 °C. A solution of CF_3COOH/CH_2Cl_2 (1:4, 117 mL) was added dropwise. The reaction mixture was stirred at room temperature for 2 h and concentrated under vacuum. The residue was dissolved in 4.0 mL of hot ethanol and precipitated with 250 mL diethyl ether. Then the solution was filtered to yield 4.96 g (10.1 mmol, 68%) as a white solid. R_f = 0.3 ($EtOH/CH_2Cl_2$ = 1:10); ^{1}H NMR (400 MHz, CD_3OD) δ 7.53-7.51 (2H, m), δ 7.42-7.32 (10H, m), δ 7.20-7.15 (1H, m), δ 7.18-7.12 (2H,

m), δ 5.22 (2H, s), δ 5.14 (2H, s), δ 3.47 (2H, t, br) δ 2.98 (3H, t, br).

***N*-(2-Aminoethyl)-2,3-bis(benzyloxy)benzamide (9).** To a solution of **8** (4.96 g, 10.1 mmol) dissolved in a sodium hydroxide solution (1.25 M, 50.0 mL) and stirred 20 min. The reaction mixture was extracted by CH_2Cl_2. The organic mixture was dried over Na_2SO_4, filtered and concentrated under vacuum. The crude product was purified by silica gel column chromatography (CH_2Cl_2/EtOH/Et_3N = 9:1:0.1, v/v/v) to yield 2.94 g (7.81 mmol, 78%) of *N*-(aminoethyl)-2,3-bis(benzyloxy)benzamide as a light yellow oil. R_f = 0.4 (CH_2Cl_2/EtOH/Et_3N = 9:1:0.1); ^{1}H NMR (400 MHz, $CDCl_3$) δ 8.11 (1H, t, br), 7.73 (1H, p, *J* = 4.4 Hz), 7,48-7.46 (2H, m), 7.43-7.33 (8H, m), 7.18-7.12 (2H, m), 5.16 (2H, s), 5.11 (2H, s), 3.33 (2H, q, *J* = 6 Hz), 2.69 (2H, t, *J* = 6 Hz), 1.34 (2H, s, br). The NMR spectrum of the final submonomer product was confirmed with the previous report.[2,3]

d. General procedure of peptoid synthesis

Using submonomer synthesis approaches with microwave heating, peptoid oligomers were synthesized under atmospheric pressure.[4] 2-Chlorotrityl chloride resin (1.14 mmol/g) was used. Typically, 0.16 mmol resin was swollen in CH_2Cl_2/DMF mixture for 30 min. The bromoacetic acid loading was performed by adding a 0.135 M solution of bromoacetic acid (0.03 g, 0.22 mmol) in DMF (1.6 mL) and *i*-Pr_2NEt (0.41 g, 3.2 mmol, 560 μL) at room temperature for 30 min. Then amine displacement step was performed by adding a 1.0 M solution of amine in DMF at room temperature for 1 h. After the first monomer was loaded, bromoacetic acid (0.44 g, 3.2 mmol, 1.2 M in DMF) and DIC (0.41 g, 3.2 mmol, 510 μL) were added to the resin and irradiated at 35 ℃ (microwave, 400 W 50% power, ramp 30 sec, hold 1 min). For amine displacement, a 1.0 M solution of amine (3.2 mmol, in DMF) was added, and the reaction mixture was irradiated at 70 ℃ (microwave, 400 W 75% power, ramp 2 min, hold 1.5 min). After each step, DMF (3×), MeOH (2×) and CH_2Cl_2 (3×) were used to wash resin. Bromoacetylation and amine displacement were repeated until the desired peptoid sequence was obtained. Cleavage from the resin was performed with CH_2Cl_2/TFE/TIS (8:1:1, v/v/v) at room temperature for 2 h and repeated thrice. The cleavage solution was concentrated by a stream of nitrogen, diluted with ACN/H_2O (1:1, v/v) solution, and filtered by Whatman Puradisc syringe filter (GE Healthcare's Life Sciences, Little Chalfont, Buckinghamshire, UK). The crude peptoid solution was lyophilized, and analyzed by ESI-MS and analytical HPLC.

General cyclization reaction.[5]

Peptoid oligomer (54.6 μmol) was dissolved in anhydrous CH_2Cl_2 (23.9 mL). 2.21 mL of a 98 mM solution of PyBOP in anhydrous CH_2Cl_2 and 2.21 mL of a 192 mM solution of *i*-Pr_2NEt in anhydrous CH_2Cl_2 were added. The reaction mixture was stirred overnight at room temperature, concentrated under vacuum and diluted with ACN/H_2O mixture. The diluted sample was filtered by Whatman Puradisc syringe filter (GE Healthcare's Life Sciences, Little Chalfont, Buckinghamshire,

UK). The crude peptoid was dissolved in ACN/H_2O, lyophilized, and analyzed by ESI-MS, and analytical HPLC.

Deprotection of acetonide on cyclic peptoids.

Acetonide groups of cyclic peptoid (64 μmol) were deprotected in a solution of TFA/H_2O/TIS (7 ml, 95:2.5:2.5, v/v/v) at room temperature for 20 min. The volatile reagents were removed by a stream of nitrogen and diluted with ACN/H_2O. The diluted sample was filtered by Whatman Puradisc syringe filter (filtered solution was frozen immediately and lyophilized to prevent oxidation of product). Deprotected peptoid was dissolved in ACN/H_2O, and analyzed by HRMS and analytical HPLC. HRMS of **1**: (ESI) m/z: $[M+H]^+$ Calculated for $C_{57}H_{61}N_6O_{12}^+$ 1021.4342; Observed 1021.4338, HRMS of **2**: (ESI) m/z: $[M+H]^+$ Calculated for $C_{45}H_{61}N_6O_{15}^+$ 925.4189; Observed 925.4187.

Deprotection of benzyl on cyclic peptoids.

Benzyl groups of cyclic peptoid (25.2 μmol) were hydrogenated using 10% Pd/C (15 mg) in MeOH (15 mL) under H_2 atmosphere at room temperature for 3 h. The resulting mixture was filtered through Celite (deoxygenated solvent was used during filtration). The solution was concentrated under vacuum and diluted with ACN/H_2O (concentrated solution was immediately diluted, frozen, and lyophilized to prevent oxidation of product). Deprotected peptoid was dissolved in ACN/water, and analyzed by HRMS and analytical HPLC. HRMS of **3**: (ESI) m/z: $[M+H]^+$ Calculated for $C_{48}H_{64}N_9O_{18}^+$ 1054.4364; Observed 1054.4364.

e. Experimental techniques

NaOH titration

The absorption of peptoid-Fe(III) complexes was observed in methanol. A solution of peptoid (100 μM, 1 equiv) and $Fe(NO_3)_3 \cdot 9H_2O$ (100 μM, 1 equiv) in ACN in a 0.5 mL quartz cuvette was titrated by gradually increasing the equivalence of NaOH (2M, aq). After 30 min incubation, the absorption was measured for each sample. Absorption spectra were obtained via Amersham Biosciences Ultrospec 2100 UV-Visible Spectrophotometer (Amersham, Little Chalfont, United Kingdom).

Et_3N titration

The absorption of **3**-Fe(III) complex was observed in ACN. A solution of **3** (100 μM, 1 equiv) and $FeCl_3$ (100 μM, 1 equiv) in ACN in a 0.5 mL quartz cuvette was titrated by gradually increasing the equivalence of Et_3N. After 30 min incubation, the absorption was measured for each sample. Absorption spectra were obtained via Amersham Biosciences Ultrospec 2100 UV-Visible Spectrophotometer (Amersham, Little Chalfont, United Kingdom).

Fluorescence titration

The fluorescence of **3**-Fe(III) complex was measured by excitation at 350 nm where the peak absorption was observed in ACN. A solution of **3** (1 equiv) and Et_3N (6 equiv) in ACN in a 2 mL quartz cuvette was titrated by gradually increasing the equivalence of iron(III) acetylacetonate (0, 0.2, 0.4, 0.6, 0.8, 1, 1.2, 1.4, 1.6, 1.8, and 2.0 equiv) (concentration of **3** was set as 100 μM). After 30 min incubation, the fluorescence was measured for each sample. Fluorescence spectra were obtained via Agilent Cary Eclipse Fluorescence Spectrophotometer (Agilent, Santa Clara, CA, USA).

EPR analysis

The electron paramagnetic resonance of **3**-Fe(III) complex was carried out at Western Seoul center, Korea Basic Science Institute (KBSI). X-band continuous-wave EPR spectrum was obtained using a Bruker EMX Plus 6/1 spectrometer equipped with a dual-mode cavity (ER4116DM). The 2 mM solution of **3** (1 equiv) with $FeCl_3$ (1 equiv) and Et_3N (6 equiv) in ACN was prepared for EPR analysis. EPR spectrum was measured with the following parameters: frequency, 9.64 GHz; power, 1 mW; modulation frequency, 100 kHz; modulation amplitude, 10 G; time constant, 40.96 ms; conversion time, 40.00 ms; sweep time, 232 s; scan, 2; temperature, 5 K.

EPR simulation

Spin Hamiltonian parameters were determined by simulating continuous wave EPR spectra with the EasySpin toolbox for MATLAB 5.2.27.[6]

DFT calculation

All calculations were performed with the Gaussian09 package using the density functional theory (DFT) with B3LYP. The LANL2DZ basis set with effective core potential (ECP) was employed for Fe atom, and the 6-31+g(d,p) basis set was employed for all other atoms. Default self-consistent reaction field (SCRF) was used for calculation in the condensed phase. The iron center was treated as high spin which has spin multiplicity as 6 (following EPR analysis).

Cyclic Voltammetry

The electrochemical measurements were done with a CH Instruments Biopotentiostat. Compounds were dissolved in anhydrous and degassed acetonitrile at 1 mM with 0.1 M tetrabutylammonium perchlorate as the electrolyte. A platinum electrode was used as the working electrode, a platinum wire was used as the counter electrode and Ag/Ag^+ electrode was used as the reference electrode. All measurements were processed in a Faraday cage.

Competitive Fe(III) binding assay

The absorption of enterobactin (Ent), deferoxamine myslate salt (DFO), deferiprone (DFP), 3,4-dihydroxybenzoic acid (3,4-DHBA), maltol, and **3** was observed at different wavelengths where the peak absorptions were observed for each metal-ligand complex in ACN/water = 9:1 mixture (Ent:510 nm, DFO:430 nm, DFP:450 nm, 3,4-DHBA:550 nm, **3**:510 nm). Absorption spectra were obtained via Biotek Cytation3 Multi-Mode Reader (Biotek, Winooski, VT, USA).

Sample preparation

Stock solutions (0.5 mM) were prepared for all chelators except DFO in ACN and DFO stock solution (0.5 mM) was prepared in ACN/water = 9:1 solution due to solubility. A stock solution of iron(III) chloride (1 mM) was prepared by dissolving anhydrous iron(III) chloride (5.8 mg) in ACN (35.8 mL). A stock solution of Et_3N (0.1 M) was prepared by dissolving Et_3N (54 µL) in ACN (3.87 mL). The stock solution of Et_3N (0.1 M) was subsequently diluted to Et_3N in ACN (10 mM). Chelators were iron-loaded by mixing chelator solution (80 µL, 0.5 mM) and iron(III) chloride solution (40 µL, 1 mM). To make a basic environment, Et_3N solution (24 µL, 10 mM) was added. A stock solution of EDTA (10 mM) was prepared by dissolving EDTA (3.9 mg) and Et_3N (1.88 µL) in water (1.35 mL). The EDTA solution was added to the metal-chelator complex solution by gradually increasing the concentration of EDTA (0, 60, 150, 240, 300, 450, 600 and 900 µM). The final concentration of all chelators and iron(III) chloride was set as 100 µM, and the solvent was ACN/water = 9:1. The solutions were prepared in 2 mL vial, and vials were incubated for 30 min, prior to measurement. Relative absorption value was determined by taking the average of triplicate the absorption value at each wavelength.

f. HPLC chromatograms

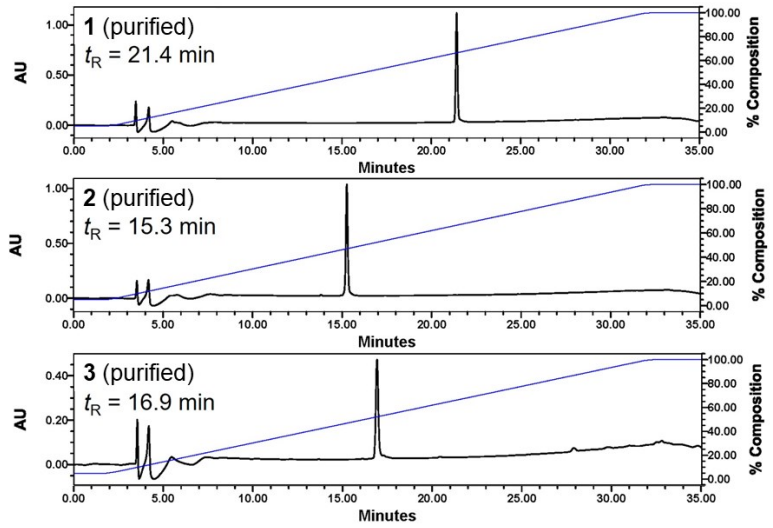

Figure S1. Analytical HPLC chromatograms of cyclic peptoids **1**–**3**. The peaks were monitored at 220 nm.

2. Spectroscopic data

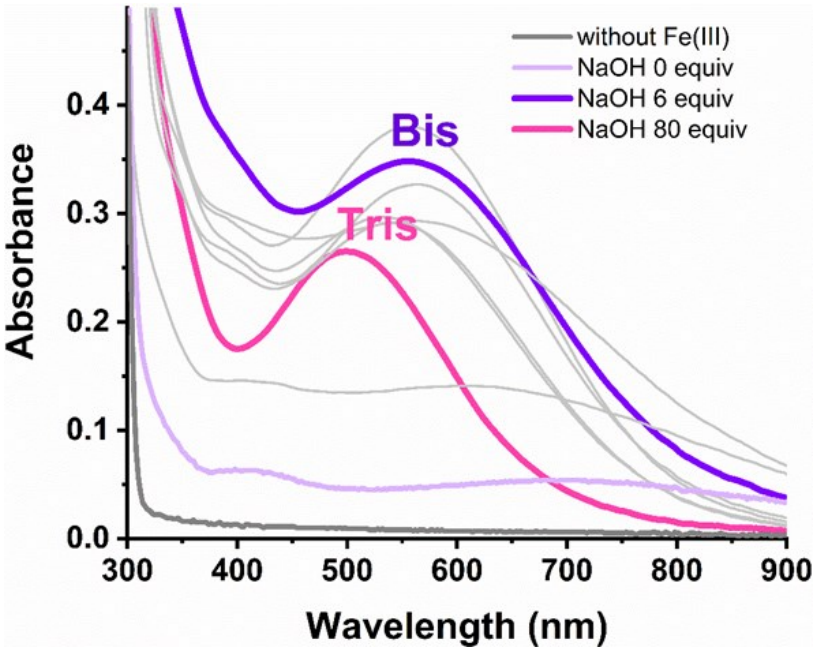

Figure S2. UV-vis spectra of a $Fe(NO_3)_3 \cdot 9H_2O$ (100 μM) and **1** (100 μM) solution in methanol titrated with NaOH.

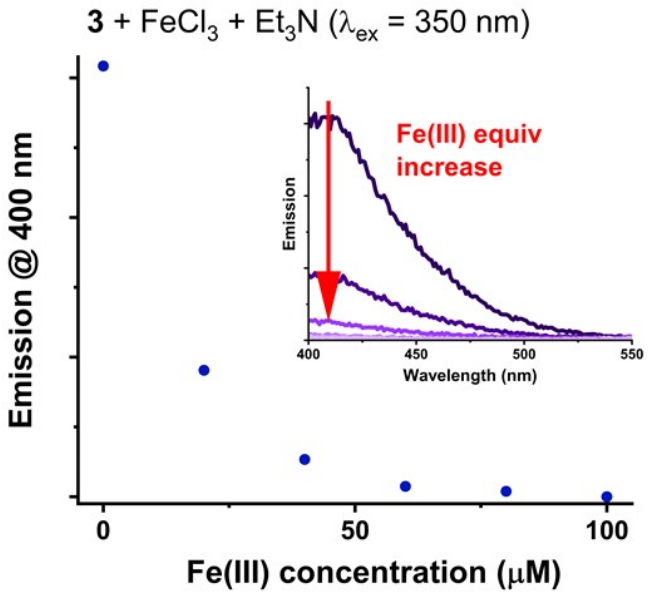

Figure S3. The plot of the fluorescence titration result for **3** (100 μM) with $FeCl_3$ in acetonitrile.

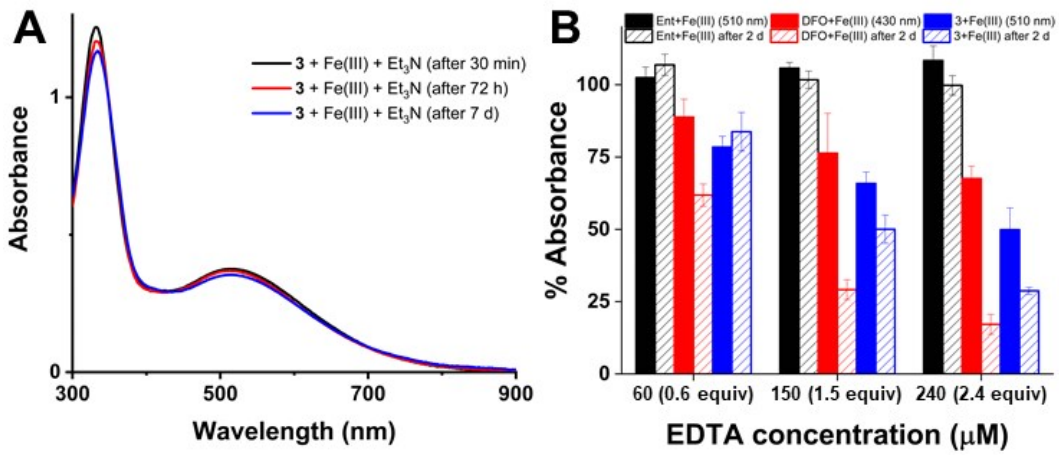

Figure S4. (A) UV-vis spectra of a $FeCl_3$ (100 μM), Et_3N (100 μM) and **3** (100 μM) solution in acetonitrile/water = 9:1 under air exposure. (B) Competitive Fe(III) binding assay with EDTA for the evaluation of iron-binding affinity. The absorbance of samples with no EDTA was set as 100%, and all samples were prepared as 100 μM in acetonitrile/water = 9:1 solution (solid bars : after 30 min incubation; dashed bars : after 2 d air exposure).

3. Electrochemistry

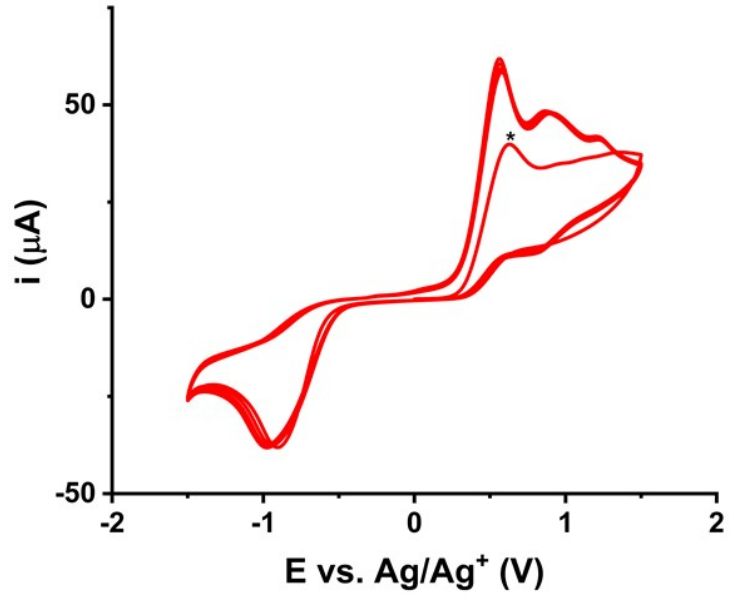

Figure S5. The plot of the cyclic voltammetry result for the **3**-Fe(III) complex (1 mM) with Et_3N (6 equiv) in acetonitrile. Tetrabutylammonium perchlorate (TBAP) was used as electrolyte (Scan rate = 0.2 V/s; Sample interval = 1 mV). *First cycle

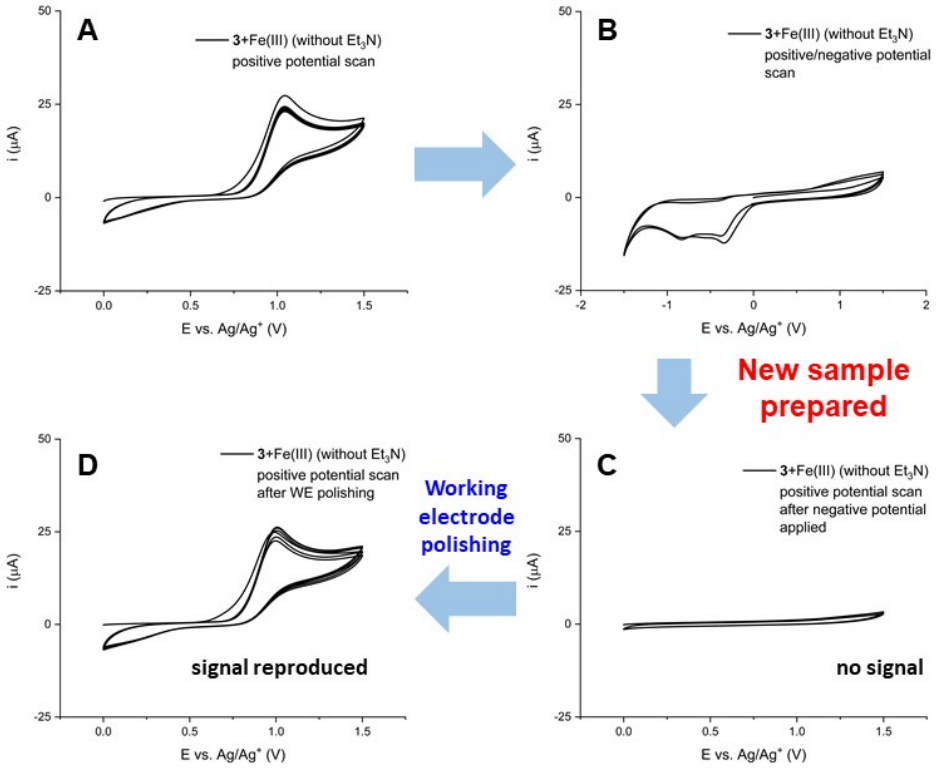

Figure S6. The plot of the cyclic voltammetry result for **3**-Fe(III) complex without base (1 mM) in acetonitrile. TBAP was used as electrolyte (Scan rate = 0.2 V/s; Sample interval = 1 mV). Positive potential scan of **3**-Fe(III) (A, C and D) / Positive and negative potential scan of **3**-Fe(III) (B)).

Reproducible cyclic voltammogram narrates the electrochemical stability of **3**-Fe(III) complex in the presence of base (i.e., Et_3N) under varied potential (Figure S5). On the other hand, **3**-Fe(III) complex without base showed no signal after coss-linking reaction occurred in the first cycle (reductive potential). Electrode with a catechol cross-linked surface was reproduced after polishing (Figure S6).

4. EPR simulation details

The EPR spectra of non-heme Fe(III) complexes are known to affected by zero-field splitting (ZFS),[7-9] and ZFS is an important parameter of local geometry. As the Zeeman hamiltonian (Eq. S1) described follow, **D** represents the spin-spin coupling between two unpaired spins while **S** is the total spin. Just like g-value also the ZFS parameter can be anisotropic and have three components D_x, D_y, and D_z. However, three components are not independent since **D** is traceless ($D_{xx}+D_{yy}+D_{zz}=0$). Therefore, they can be reduced to two independent components D and E (Eq. S2). D represents the axial component of the coupling interaction, and E represents the transverse component.

$$H_{spin} = H_{Zeeman} + H_{ZFS} = g\beta \mathbf{B} \cdot \mathbf{S} + \mathbf{S} \cdot \mathbf{D} \cdot \mathbf{S} \quad \text{(Eq. S1)}$$

$$H_{ZFS} = \mathbf{S} \cdot \mathbf{D} \cdot \mathbf{S}$$

$$= D_x S_x^2 + D_y S_y^2 + D_z S_z^2$$

$$= \frac{3}{2} D_z \left(S_x^2 - \frac{S(S+1)}{3} \right) + \frac{(D_x - D_y)}{2} \left(S_x^2 - S_y^2 \right) = D \left(S_x^2 - \frac{S(S+1)}{3} \right) + E \left(S_x^2 - S_y^2 \right) \quad \text{(Eq. S2)}$$

The rhombicity η (= E/D) narrates the local geometry of the metal complex. The axial complex has no distinctiveness of the transversal splitting parameter, therefore, E/D = 0. On the other hand, the rhombic complex has non-zero rhombicity. Moreover, the value of rhombicity affects the 'effective' g value which is an apparent g value. Particularly the effective g value is dependent under E/D value (Eq. S3-S5).[10]

$$g_x^{eff} = g_x \left[\left(\frac{15}{7} \right) - 60 \left(\frac{102}{2401} \right) \left\{ \frac{1 - \frac{3E}{D}}{1 + \frac{E}{D}} \right\}^2 \right]$$

$$g_y^{eff} = g_y \left[\left(\frac{15}{7} \right) - \frac{\left(\frac{60}{49} \right) \left(1 - \frac{3E}{D} \right)}{1 + \frac{E}{D}} \right] \quad \text{(Eq. S3)}$$

$$g_z^{eff} = g_z \left[\left(\frac{15}{7} \right) - \frac{\left(\frac{60}{49} \right) \left(1 - \frac{3E}{D} \right)}{1 + \frac{E}{D}} \right] \quad \text{(Eq. S4)}$$

(Eq. S5)

The simulation was provided with the restrain factor; real g value, ZFS parameters *D* and *E* were

simulated with strained variation (real g_x, g_y, and g_z values were calculated with Eq. 3-5). The function 'pepper' was used for the high-spin environment (S > 1/2) and 'esfit' fitting was used for the least-squares fitting of EPR spectra. Monte Carlo method was used, and data was targeted as is. The initial condition was calculated with Eq. 3-5 (for real g values) and rhombogram (for D and E value). The simulation was started at the center of the range and proceeded. In result, ZFS parameters were found out to be D = 0.231 cm^{-1}, E = 0.071 cm^{-1} and the rhombicity $\eta = 0.31$.

In the previous report, rhombicity was defined within a range of 0 to 1/3.[11] The rhombicity of **3**-Fe(III) ($\eta = 0.31$) showed similarity with enterobactin (pure rhombic, $\eta = 0.33$),[9,12] which defined **3**-Fe(III) complex to be partially rhombic non-heme iron complex.

5. DFT calculation

The crystal structure of cyclic peptoid hexamer[13] was used as the initial geometry of the peptoid backbone, and side chains were varied as the catecholate chelating arms. The vibrational frequencies were computed at the same level and there was no negative (imaginary) frequency.

Z-matrix of DFT calculated compounds

Coordination of **3**-Fe(III) complex

O	11.53456	9.34718	11.21669	N	8.86931	2.83291	12.14511
N	9.89948	7.86583	10.5692	C	10.1271	1.95254	14.1277
C	10.71993	7.85899	12.92624	O	7.52402	8.24844	11.92678
O	11.74849	5.48282	12.14261	N	6.9454	6.0251	11.94226
N	12.05032	7.39172	13.36457	C	7.24503	4.62728	11.63801
C	10.74641	8.3982	11.49478	C	8.39645	4.06782	12.48717
O	13.34076	1.92106	13.59722	C	9.06574	6.69633	10.85226
N	13.89302	4.12987	13.3073	C	7.78899	7.05367	11.6208
C	13.68787	5.5468	13.6213	C	5.66058	6.34137	12.59617
C	12.436	6.14526	12.96603	C	4.55156	6.56193	11.57392
C	12.85457	8.2958	14.20956	O	12.71913	7.00242	16.25009
C	12.43241	8.308	15.67466	O	4.31448	5.29691	10.89109
C	11.93729	3.5488	14.73809	C	11.09896	1.79435	16.36488
C	13.11268	3.13935	13.8343	C	12.0351	0.57431	16.36881
O	9.29197	1.05622	14.43454	O	12.05794	-0.05781	17.68325
N	11.02828	2.43842	15.03851	C	12.31771	6.88436	17.64433
C	10.18792	2.46802	12.69093	C	12.97462	0.55937	18.63226
O	8.93311	4.75407	13.3997	C	3.63074	5.44181	9.6127

C	9.87424	8.49833	9.22744	H	10.43123	8.69351	13.57006
C	8.55281	8.3387	8.47265	H	10.00625	7.05335	13.08215
N	8.44703	7.03719	7.81248	H	14.57319	6.08958	13.2807
C	7.2808	6.59142	7.26058	H	13.61597	5.70587	14.7028
C	7.37411	5.36179	6.43569	H	12.75311	9.30254	13.79399
C	8.55962	4.59127	6.33528	H	13.90978	8.02751	14.13521
C	6.25629	5.01442	5.63493	H	12.99449	9.08847	16.20767
C	8.64684	3.55249	5.34691	H	11.36074	8.5318	15.77641
C	6.32645	3.96327	4.72761	H	12.33184	3.92694	15.68666
C	7.52724	3.23931	4.5692	H	11.36049	4.3583	14.28867
O	6.19578	7.24647	7.40258	H	10.60933	1.67252	12.07362
O	9.67184	4.77703	7.0848	H	10.82995	3.33901	12.5737
O	9.84645	2.93826	5.23982	H	6.32803	4.05394	11.78477
C	15.06073	3.72898	12.48509	H	7.4976	4.51235	10.57737
C	14.74862	3.11683	11.1062	H	8.79506	6.2368	9.89846
N	14.29512	4.03216	10.06204	H	9.66812	5.96604	11.39476
C	15.14344	4.90858	9.44916	H	5.39877	5.51816	13.26598
C	14.70279	5.48362	8.15157	H	5.79309	7.24757	13.1902
C	15.56894	6.40015	7.50191	H	4.8605	7.32865	10.85082
C	13.52657	5.06077	7.48219	H	3.63151	6.90321	12.07052
C	15.29644	6.85473	6.21693	H	10.0942	1.47068	16.64193
C	13.29227	5.4718	6.12272	H	11.43439	2.54208	17.08861
C	14.16462	6.38078	5.51717	H	11.65419	-0.18332	15.68024
O	16.2924	5.16264	9.94409	H	13.04769	0.85345	16.05381
O	12.5974	4.23507	8.00815	H	12.85258	7.60962	18.27096
O	12.21208	4.92613	5.51406	H	11.23705	7.03953	17.75681
C	8.04768	1.9046	11.32156	H	12.57631	5.87162	17.9548
C	8.68779	0.55326	11.02203	H	12.68082	1.58595	18.8834
N	9.75323	0.64676	10.02769	H	12.93641	-0.05341	19.53431
C	10.55417	-0.4254	9.75198	H	13.9997	0.56775	18.23883
O	10.45976	-1.49847	10.43245	H	2.64755	5.91474	9.73776
C	11.50275	-0.28163	8.62164	H	4.23545	6.03308	8.91293
C	12.3478	-1.38418	8.33278	H	3.49878	4.43221	9.22067
C	11.56997	0.87719	7.80664	H	10.07682	9.56046	9.38034
C	13.23338	-1.34624	7.26368	H	10.70308	8.10596	8.62144
C	12.48791	0.90569	6.69709	H	8.49698	9.14073	7.72267
C	13.30196	-0.20196	6.44061	H	7.70255	8.4855	9.14577
O	10.81214	1.98621	7.97654	H	9.26961	6.43936	7.6627
O	12.50737	2.03777	5.95864	H	5.35566	5.61017	5.73481
Fe	11.26011	3.49544	6.57906	H	5.46212	3.70945	4.12021

H	7.60345	2.44078	3.83621	H	7.79407	2.39062	10.37216
H	15.69507	4.60396	12.34698	H	9.06695	0.09564	11.94046
H	15.6229	2.97871	13.05294	H	7.8865	-0.10677	10.65844
H	15.68161	2.63677	10.7765	H	9.85161	1.45281	9.39716
H	13.99622	2.33486	11.21865	H	12.27356	-2.25685	8.97193
H	13.40845	3.86546	9.57468	H	13.8745	-2.19823	7.05469
H	16.46287	6.71266	8.03024	H	13.98645	-0.16291	5.59742
H	15.96732	7.56094	5.73537				
H	13.96777	6.70107	4.4976				
H	7.10841	1.71059	11.85219				

6. NMR spectra

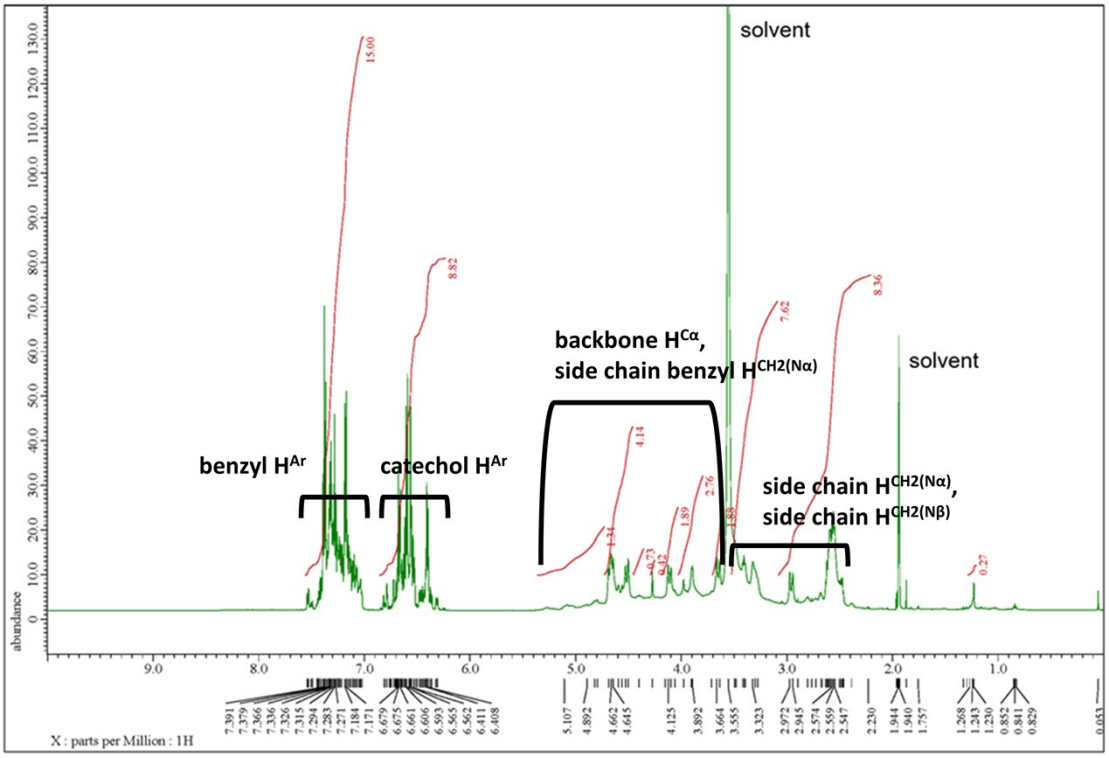

Figure S7. ^{1}H NMR spectrum of **1** at 600 MHz in CD_3CN/D_2O = 5:1.

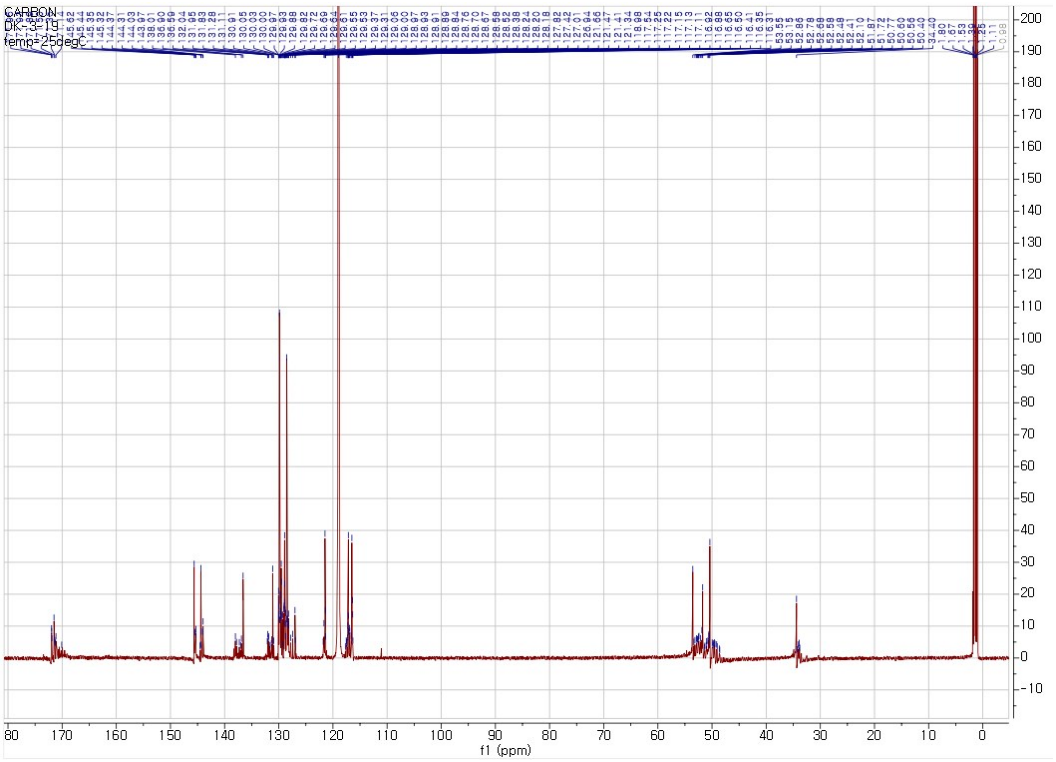

Figure S8. ^{13}C NMR spectrum of **1** at 600 MHz in CD_3CN/D_2O = 5:1.

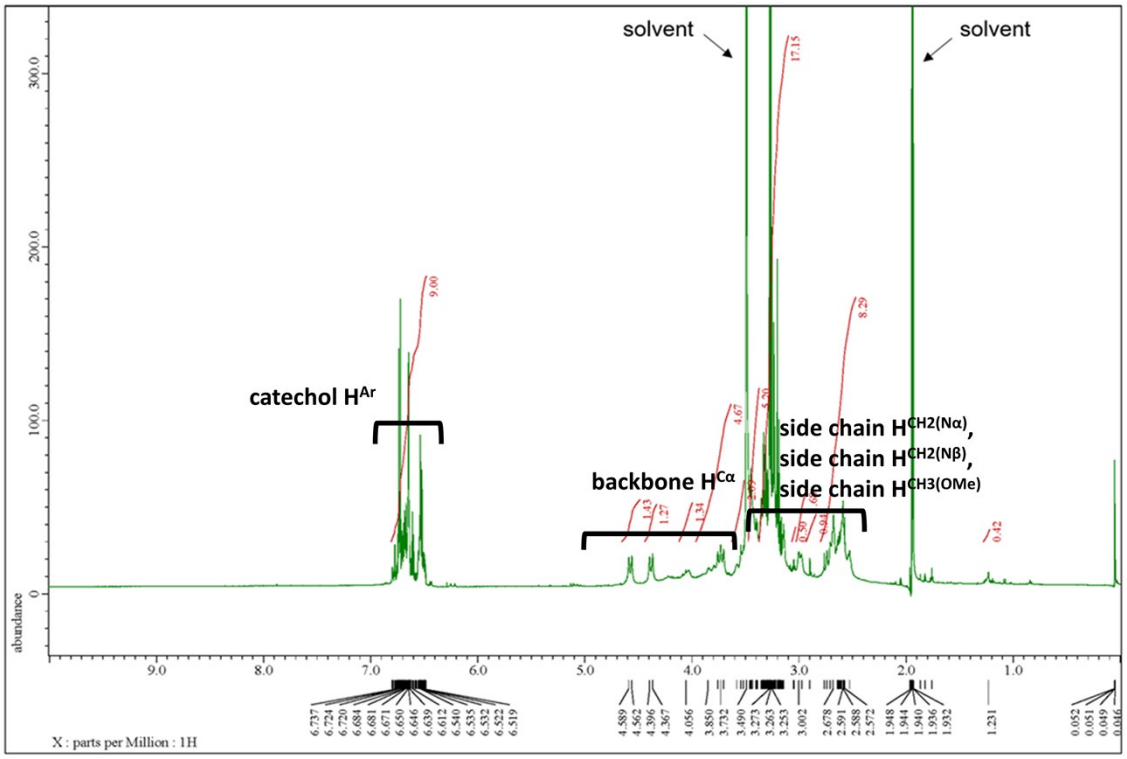

Figure S9. ^{1}H NMR spectrum of **2** at 600 MHz in CD_3CN/D_2O = 5:1.

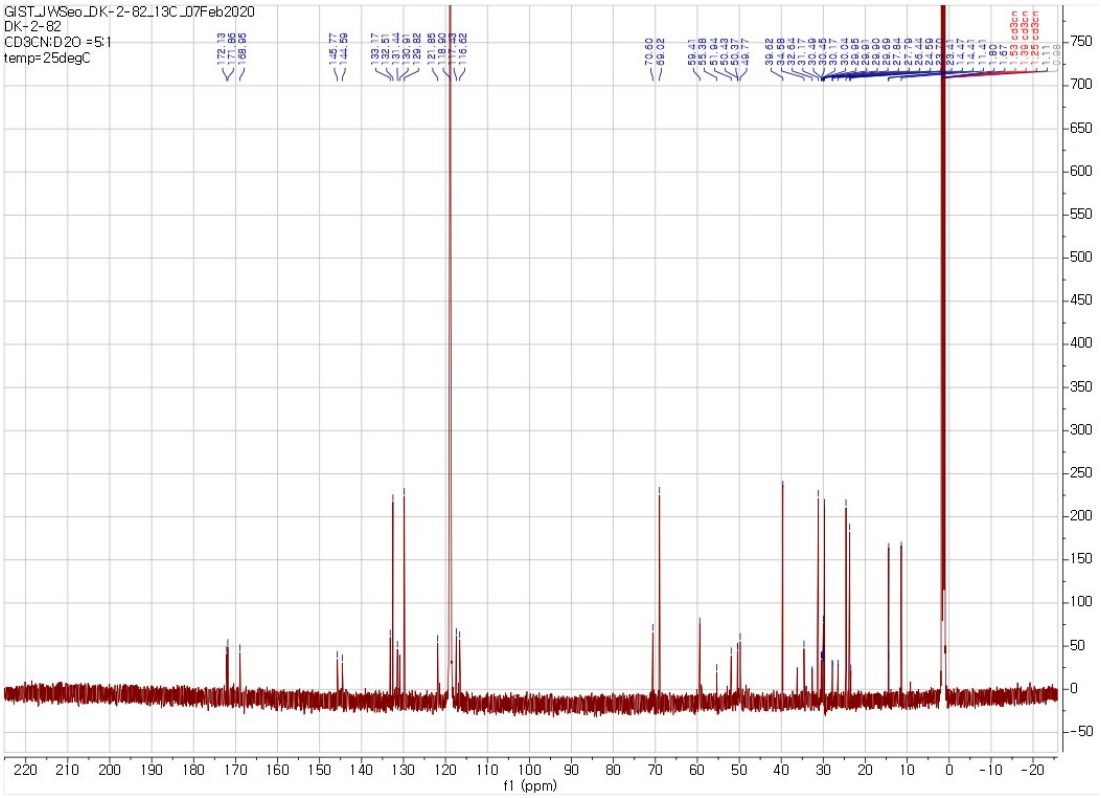

Figure S10. ^{13}C NMR spectrum of **2** at 600 MHz in CD_3CN/D_2O = 5:1.

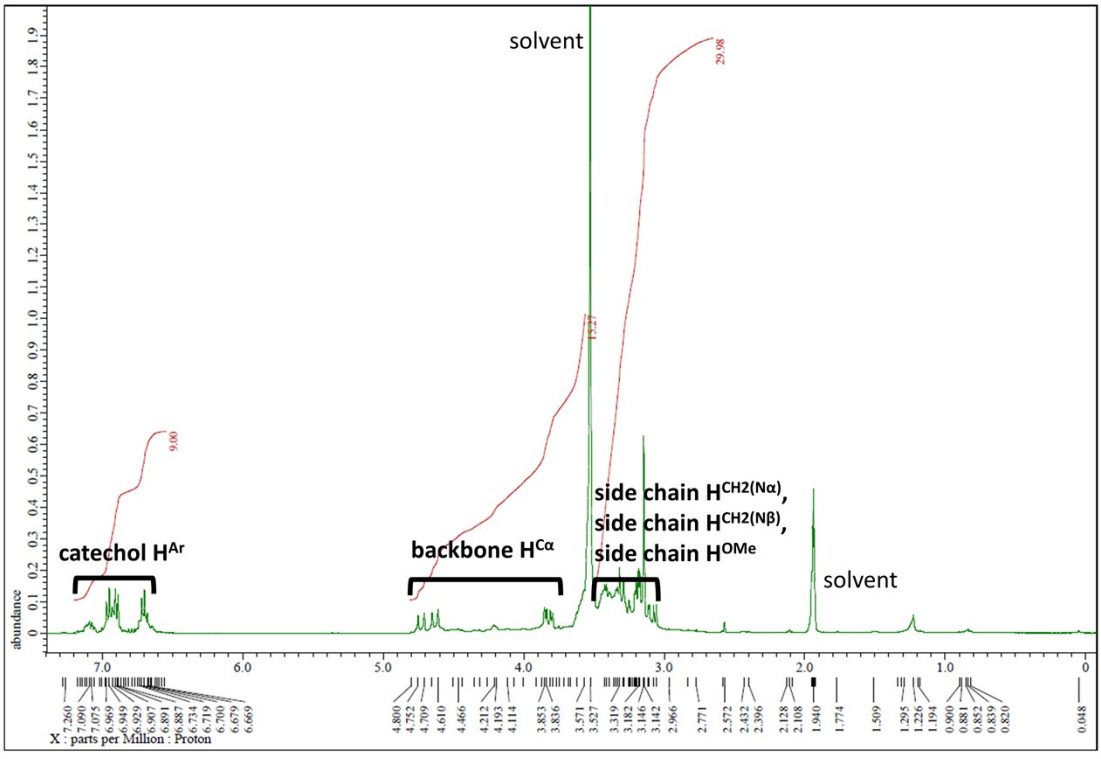

Figure S11. ^{1}H NMR spectrum of **3** at 400 MHz in CD_3CN/D_2O = 5:1.

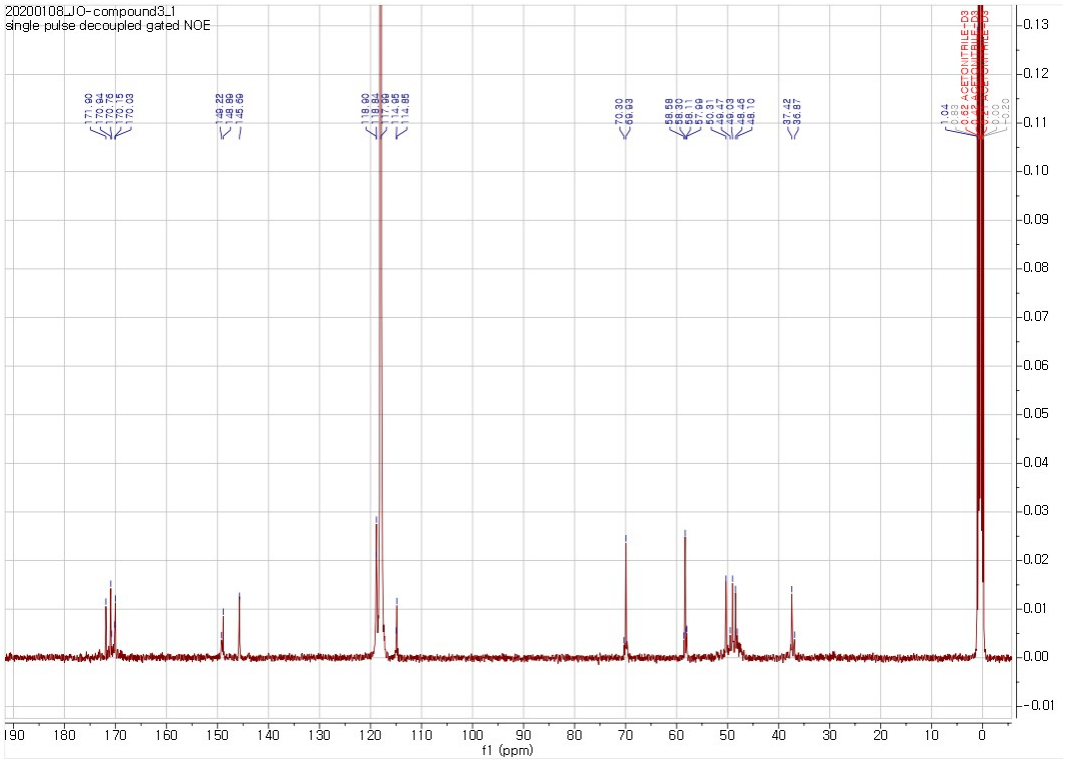

Figure S12. ^{13}C NMR spectrum of **3** at 400 MHz in CD_3CN/D_2O = 5:1.

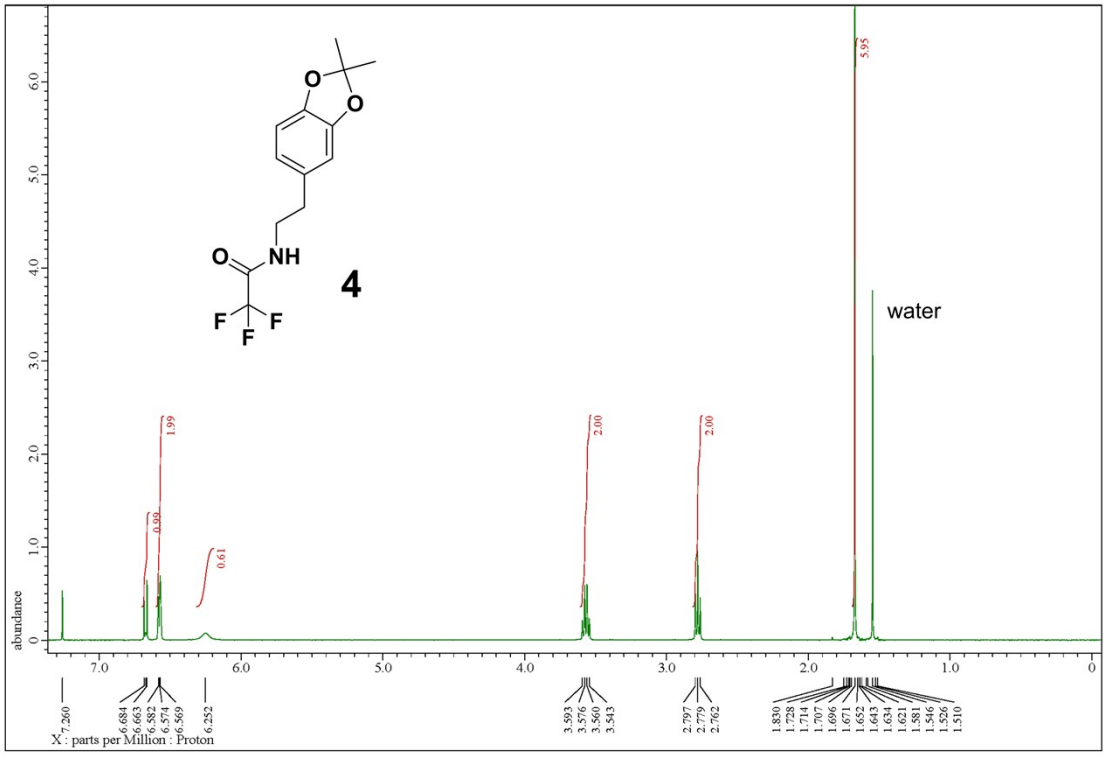

Figure S13. ^{1}H NMR spectrum of **4** at 400 MHz in $CDCl_3$.

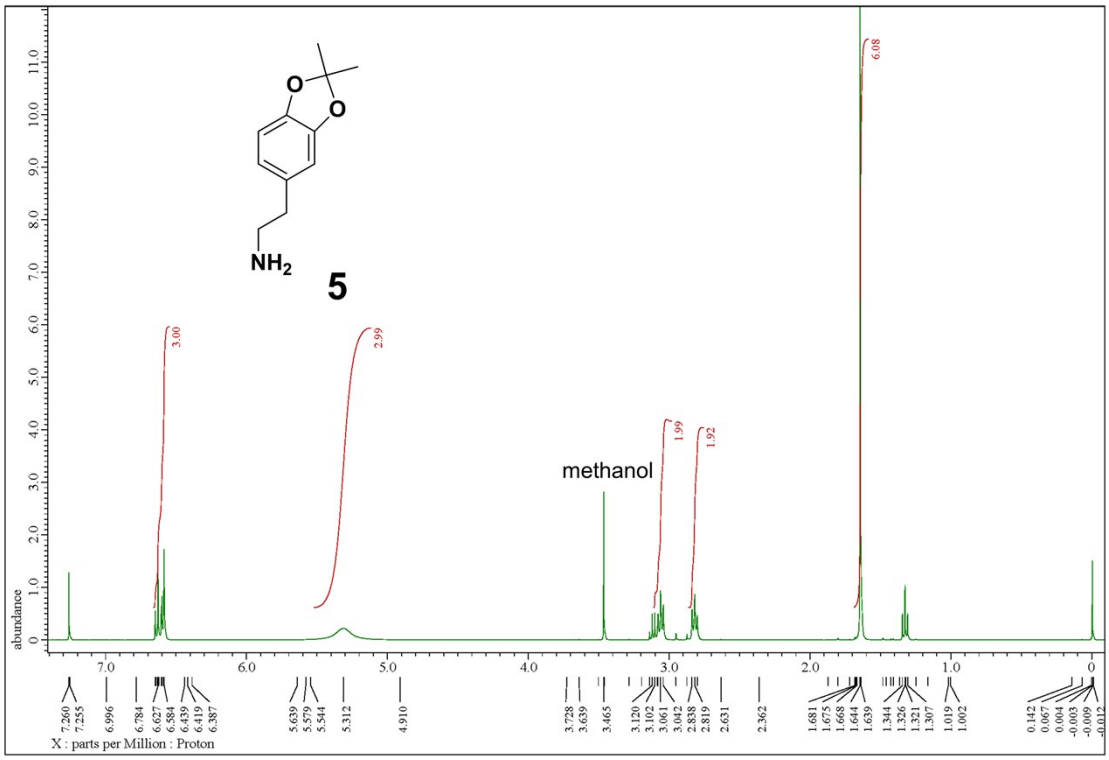

Figure S14. ^{1}H NMR spectrum of **5** at 400 MHz in CD_3OD.

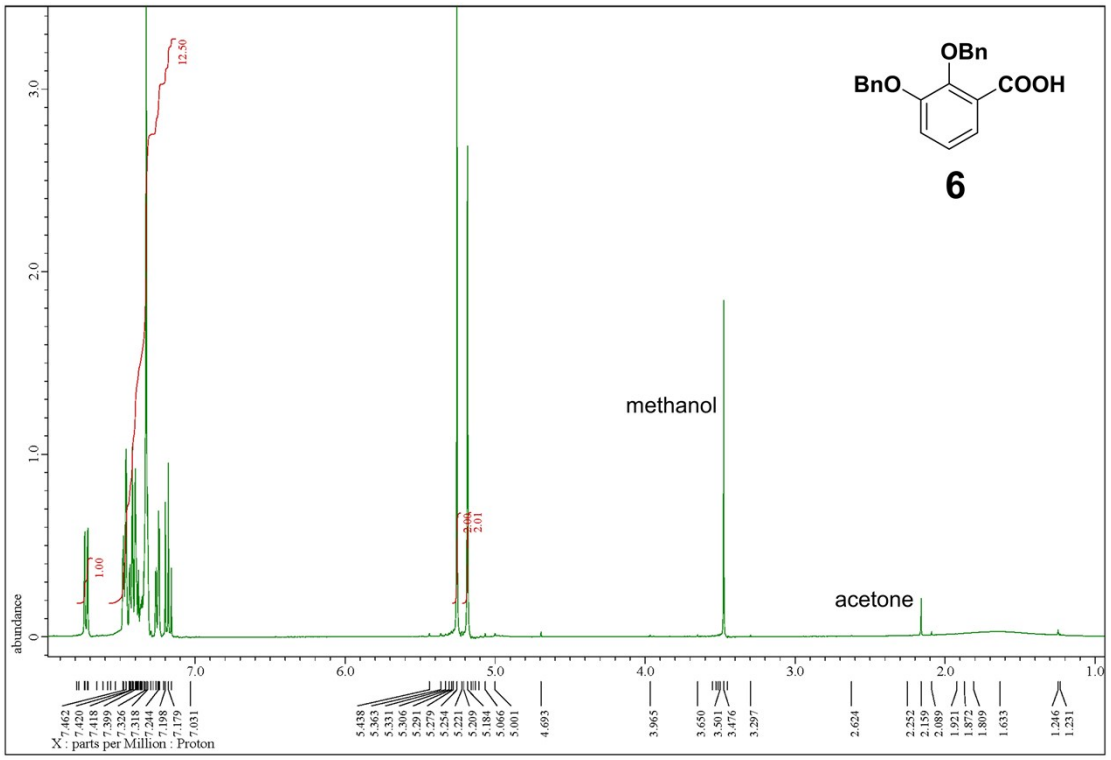

Figure S15. ^{1}H NMR spectrum of **6** at 400 MHz in CD_3OD.

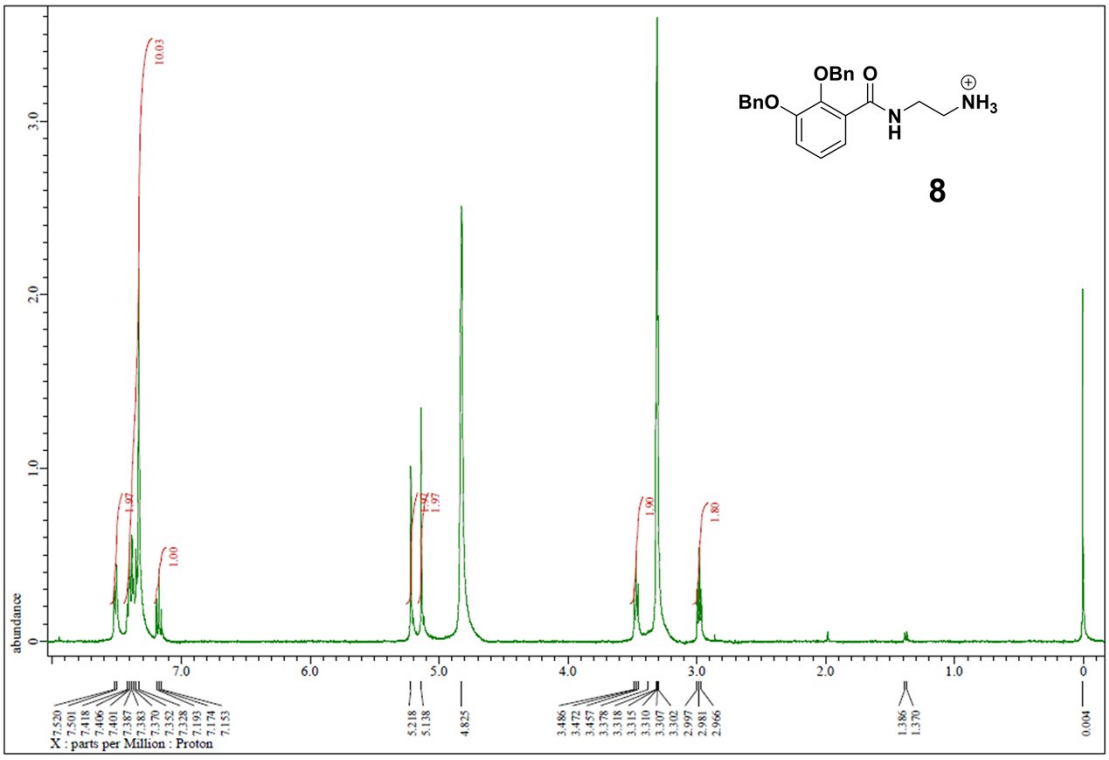

Figure S16. ^{1}H NMR spectrum of **8** at 400 MHz in CD_3OD.

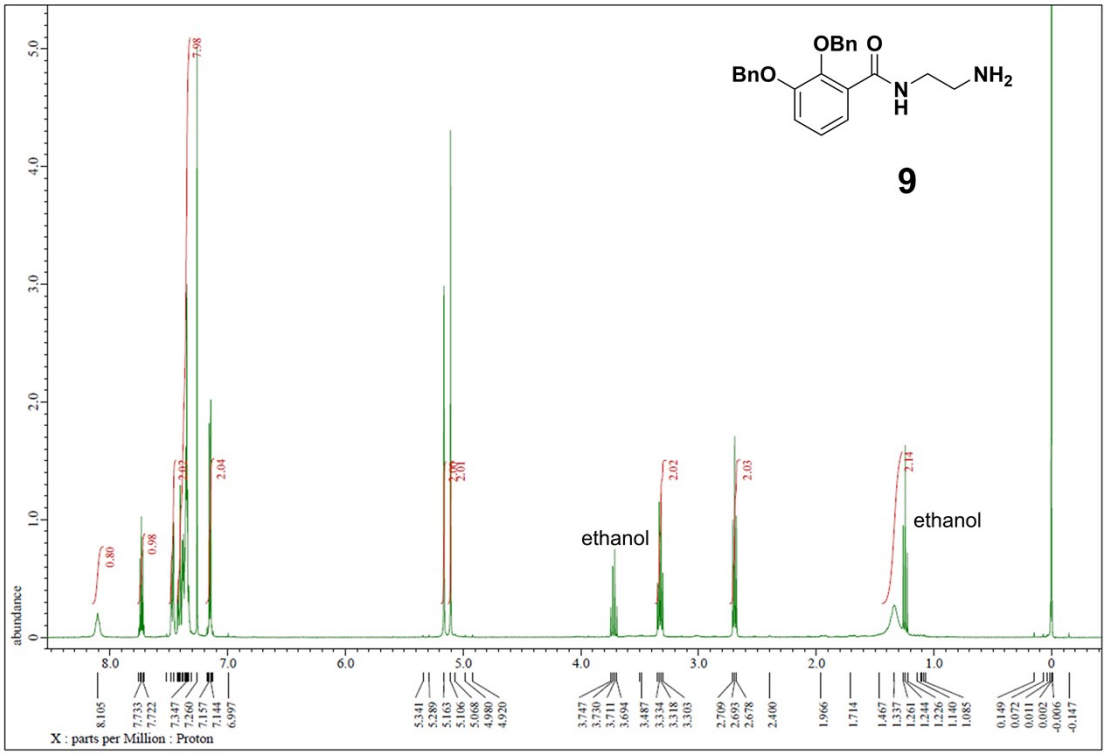

Figure S17. ^{1}H NMR spectrum of **9** at 400 MHz in $CDCl_3$.

7. HRMS spectra

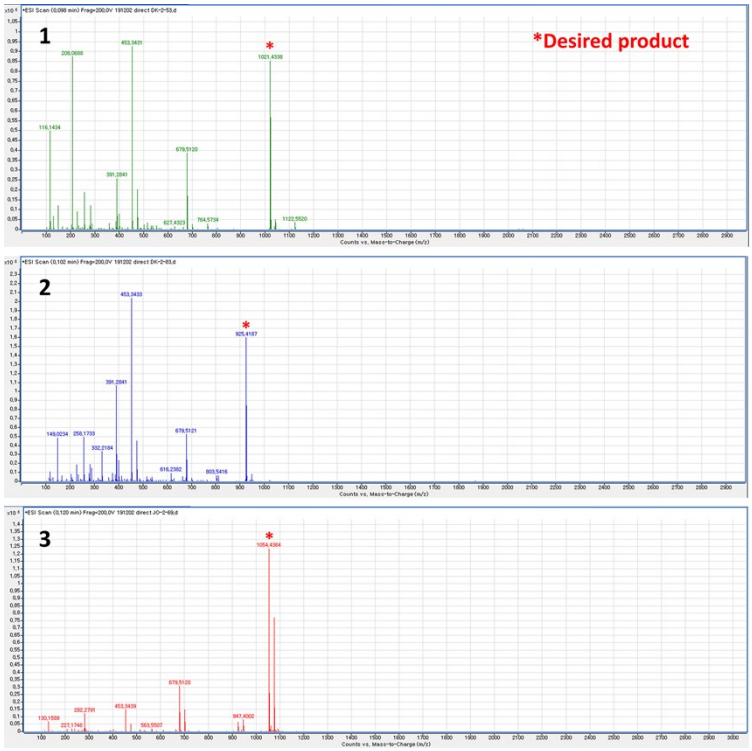

Figure S18. HRMS spectra of **1**–**3**

8. References

(1) Z. Liu, B.-H. Hu and P. B. Messersmith, *Tetrahedron Lett.*, 2010, **51**, 2403-2405.

(2) R. A. Gardner, R. Kinkade, C. Wang and Phanstiel, *J. Org. Chem.*, 2004, **69**, 3530-3537.

(3) S. Lei, B. Jin, Q. Zhang, Z. Zhang, X. Wang, R. Peng and S. Chu, *Polyhedron*, 2016, **119**, 387-395.

(4) R. N. Zuckermann, J. M. Kerr, S. B. H. Kent and W. H. Moos, *J. Am. Chem. Soc.*, 1992, **114**, 10646-10647.

(5) S. B. Y. Shin, B. Yoo, L. J. Todaro and K. Kirshenbaum, *J. Am. Chem. Soc.*, 2007, **129**, 3218-3225.

(6) S. Stoll and A. Schweiger, *J. Magn.*, 2006, **178**, 42-55.

(7) H. H. Wickman, M. P. Klein and D. A. Shirley, *Chem. Phys.*, 1965, **42**, 2113-2117.

(8) C. Bagyinka, L. Horváth and L. Keszthelyi, *Acta Phys. Hung.*, 1984, **55**, 185-194.

(9) F. Bou-Abdallah and N. D. Chasteen, *J. Biol. Inorg. Chem.*, 2008, **13**, 15-24.

(10) R. Aasa, *J. Chem. Phys.*, 1970, **52**, 3919-3930.

(11) D. R. Hutton and G. J. Troup, *Br. J. Appl.*, 1964, **15**, 275-280.

(12) K. Spartalian, W. Oosterhuis and J. Neilands, *Chem. Phys.*, 1975, **62**, 3538-3543.

(13) C. Tedesco, E. Macedi, A. Meli, G. Pierri, G. Della Sala, C. Drathen, A. N. Fitch, G. B. M.

Vaughan, I. Izzo and F. De Riccardis, *Acta Crystallogr. B*, 2017, **73**, 399-412.